RSC Advances

ROYAL SOCIETY OF CHEMISTRY

www.rsc.org/advances

Mechanistic Insights of SrtA-LPXTG Blockers targeting the transpeptidase mechanism in *Streptococcus mutans*

Chandrabose Selvaraj[1], Ramanathan Bharathi Priya[2], Jung-Kul Lee[1], Sanjeev Kumar Singh[2]*

[1]*Department of Chemical Engineering, Konkuk University, 1 Hwayang-dong, Gwangjin-gu, Seoul, Korea, Postal Code: 143-701*

[2]*Department of Bioinformatics, Computer Aided Drug Design and Molecular Modeling Lab, Science Block, Alagappa University, Karaikudi, Tamilnadu, India*

Address correspondence
Dr. Sanjeev Kumar Singh,
Associate Professor,
Department of Bioinformatics,
Computer Aided Drug Design and Molecular Modeling Lab,
Alagappa University, Karaikudi-630003,
Tamil Nadu, India

Tel: + 91-4565-230725.
Fax: + 91-4565-225202.
E-mail: skysanjeev@gmail.com

Key Words: Streptococcus mutans; Dental caries; Sortase A; LPXTG; Transpeptidation; Molecular Dynamic Simulation

Abstract

Streptococcus mutans has been chiefly involved as the major etiological agent of dental caries and adherence to the tooth surface for dental plaque formation occurs through cysteine transpeptidase sortase A (SrtA) mediated covalent anchoring of surface proteins. SrtA recognizes the LPXTG sequence substrate located in C-terminus of surface proteins and also acts as a decisive therapeutic target for the development of novel antimicrobial agents. Recent experimental studies have defined the role of fully conserved Leu and Pro residues of LPXTG substrate in modulating dynamics of SrtA structure. Therefore, in the present work, we have examined the invariant Leu residue of the substrate with a view to understand its role in altering the dynamics of enzyme substrate complex structure using molecular dynamic simulations and energy calculation method, while the results revealed that Leu residue of the substrate appears to play the crucial role in anchoring and directing the conformational transition of the enzyme. In addition to that, we have identified the potential lead compounds which target the Leu residue of substrate as peptide blockers to impede SrtA-mediation transpeptidation reaction. Hence, this approach provides a new platform for therapeutic drug targeting and rational design of inhibitors against the bacterial infections.

Introduction

Streptococcus mutans is the well-known biofilm-forming organism ubiquitously associated with dental caries in human and animal species [1-2], one of the most common chronic infectious diseases that affect a large number of populations in the world [3]. This Gram-positive bacterium has evolved a biofilm lifestyle for survival and persistence in its natural environment, dental plaque [4]. Generally, LPXTG motif-containing surface proteins are critically important in determining the success of a bacterial strain in its competition for survival in the world and several cell wall-anchored surface proteins are involved in the adherence of bacteria to tooth surface or to other streptococci and actinomycetes that are present in mixed biofilms and in dental plaque [5-7]. While an analysis of the *S. mutans* UA159 genome indicates that it encodes six proteins P1 (-antigen I/II), fructanase (-FruA), wall-associated protein A (-WapA), wall-associated protein E (-WapE), glucan-binding protein C (-GbpC) and dextranase (-DexA) containing the LPXTG motif located at the C-terminus followed by hydrophobic region and positively charged tail plays an important role in pathogenicity [8]. Among these LPXTG-containing surface proteins FruA, WapA and WapE are involved in biofilm formation and the cell wall covalent anchoring transpeptidation reaction was catalyzed by the housekeeping class A enzyme sortase (SrtA) [9-10], which cleaves the peptide bond between the threonine and glycine residues in the LPXTG motif and links the threonine to amino group of pentaglycine cell wall cross bridge, thus forming the cell wall attached protein [11-12]. Over the past decade, the oral pathogen *S. mutans* SrtA-mediated surface proteins attachment have been studied extensively for their role in oral colonization [13]; therefore, SrtA has attracted great interest as potential drug targets in terms of understanding a cariogenic dental pathogen infection process and could become a promising key target for all the Gram-positive bacteria [14-15]. Recent studies have implicated that invariant Leu residue of the substrate appears to play crucial role of an anchor and induced the direct conformational change of enzymes in an induced-fit fashion, whereas substrate Pro residue facilitates stabilization of bound pentapeptide conformation more efficiently to the enzyme active site [16]. In contrast, lack of active sortase A or LPXTG may lose the biological function mediated by these bacterial cell surface proteins [17].

The overall mechanism of SrtA-LPXTG and importance of LEU residue is explained in the Figure 1. Specifically by targeting LEU residue of LPXTG substrate and blocking the SrtA-mediated transpeptidation mechanism. 1**a)** Highly active screened peptide blocker compounds bound to Leu of substrate and SrtA enzyme. **1b)** Sortase A involved in covalent anchoring of surface protein to the cell envelope of Gram-positive bacteria. (Leu residue of

LPXTG motif cell wall anchor domain protein distinctly contribute towards anchoring and conformation of the SrtA) **1c)** Screened peptide blocker lead compound bound between the active site of SrtA and NH_3 group of substrate Leu residue alter the anchoring conformation of enzyme and thereby hinder the SrtA-catalyzed transpeptidation reaction. **1d)** Single-point (atom) mutational changes at the residue of Leu H1, H2 and H3 atoms of NH_3 was replaced with methyl group induce the specific conformational changes in protein structure. The overall figure illustrates the importance of the study and therefore we explored the characteristic of the conformational and energy level changes in active SrtA-LPXTG complex to define the role of fully conserved Leu residues of the substrate in modulating the dynamics of protein. In addition to that, we have also tried to identify inhibitors which specifically interacted with Leu of pentapeptide to block SrtA-mediated transpeptidation reaction. Thence, this novel practice has importance in designing SrtA inhibitor for the therapy of Gram-positive bacterial infection.

Material and Methods

All computational analyses were carried out using commercial version of Schrodinger software package, LLC; New York, NY 2015, and academic version of Desmond molecular dynamics package on a CentOS v.6.3 Linux platform in GPU workstation on an Intel Xeon E5620 processor.

Homology modeling and molecular docking

The catalytic domain (From Gln 66 to Glu 202) of *S. mutans* SrtA was modeled by homology modeling using appropriate templates. The protein sequence of *S. mutans* SrtA enzyme was retrieved from UniPort database (Accession number: Q7WT43) and BLASTP search was performed with default parameters against the Brookhaven Protein Data Bank (PDB) to find appropriate template structure for the calculations of homology modeling. Based on the identity and e-value scores, the structure of PDB ID-3RCC (SrtA from *Streptococcus agalactiae*) and PDB ID- 2KW8 (SrtA from *Bacillus anthracis*) were chosen as suitable templates, while the homology model is constructed by modeller 9v10 software based on a given aligned sequence and templates [18-19]. The model protein structures were ranked based on the internal scoring function (DOPE score) and least internal score model was selected for validation analysis [20]. Minimization of protein is performed until the average RMSD of non-hydrogen reached 0.3 Å even though the model structure is prepared through protein preparation wizard. Here, the chemical accuracy was ensured by addition of

hydrogen atoms, correcting the bond orders and by neutralizing the side chains that were neither close to the binding cavity nor involved in the formation of salt bridges. [21]. Meanwhile, the quality of predicted least energy refined (optimized and minimized) protein structure model was evaluated to check dihedral angle distribution using Ramachandran plot in the PROCHECK [22] and Non-Local Environment (NLE) energy calculation of each heavy atom on a protein chain was performed using Atomic Non-Local Environment (ANOLEA) to calculate energy value for each amino acid of the protein [23-24]. In addition to that, the ProSA tool was used to check potential errors of the overall modelled protein structure [25]. Finally, the refined model is further subjected into other molecular modelling studies.

To dock the LPXTG motif in the *S. mutans* SrtA, an LPNTG (X= asparagine (N)) was constructed by chimera v1.8.1, optimized through LigPrep 3.4 module in maestro 10.2 using the OPLS-2005 force field and docked into predicted active site of the SrtA homology model using extra precision Grid-Based Ligand Docking with Energetics (Glide) software from Schrodinger v10.2 package [26], which docks ligand flexibly and generates conformation internally and passes these through series of filters [27]. At last, the lowest-energy of docked complex was selected for subsequent MD simulation and energy calculation studies. Additionally, to describe the role of conserved leucine residue of the substrate in binding and dynamic state of SrtA substrate complex. We prepared mutant LPNTG substrate by specifically altering the different points of Leu NH_3 groups (amino H1, H2 and H3) into functional methyl group as single-point (atom) mutations using ligand functional group mutation module in Desmond package.

Energy calculations

Molecular electrostatic potential (MESP) calculation

The high-level all quantum chemistry calculation for native and mutated LPNTG peptides was performed using the density functional theory (DFT) method. All DFT computations were carried out using hybrid DFT with Becke's three-parameter exchange potential and the Lee–Yang–Parr correlation functional (B3LYP), using the basis set 6-31G** level [28-29]. The quantum chemical descriptors, including Molecular electrostatic potential (MSEP), Highest Occupied Molecular Orbitals (HOMOs), Lowest Unoccupied Molecular Orbitals (LUMOs) and aqueous solvation energy, were computed through single-point energy calculation in Jaguar [30]. The electrostatic potentials surface was created

through poisson-Boltzmann (APBS) method over the substrate to provide a measure of the electrostatic potential at roughly the van der Waals surface of the molecules.

Free energy Perturbation Calculation

Molecular dynamics free energy perturbation calculation was used to estimate the relative free energy state value of mutant LPNTG peptide, while mutant LPNTG substrate obtained through single-point mutation of leucine H1 and H2 atoms of NH_3 were replaced with methyl group were included for computing substrate free energy difference values. The free energy was obtained with the solvent environment and production simulations were run for 10.0 ns using 10Å buffer with solvent SPC water model under NPT ensemble at constant temperature (300K).

Virtual Screening of Peptide Blocker Compounds

Structure-based screening of optimized compounds from zinc database was performed to identify potential ligand molecules that interact with druggability regions of the SrtA with peptide complex structure. The screened compounds were docked through filtering criteria of HTVS, SP and XP docking. After ensuring the suitability of protein peptide complex and ligand for docking, the receptor grid file is generated using a grid-receptor generation program [31]**.** To soften the potential for non-polar part of receptor, we scaled Van der Waal radii of receptor atoms by 1.0 Å with a partial charge cutoff 0.25. The docking based screening includes three different phase and in each phase; the best compounds are chosen for next phase based on the scoring parameters. The compounds with less scoring parameters were eliminated at each docking phase and compounds with better scoring are passed to the next phase of docking. Glide XP mode determines all reasonable conformations for each low energy conformer in the designated binding site. In this process, the torsion degrees of each ligand were relaxed, though the protein conformation was fixed. During the docking process, the Glide scoring function (G-score) was used to select the best conformation for each ligand. The final energy evaluation was done with Glide score and a single best pose is generated as output for a particular ligand.

Molecular Docking through Multiple Conformations of Protein

Although screening is performed with the rigid receptor peptide complex and flexible ligand molecules, here we endeavor different flexible conformations of protein peptide complex by using Induced Fit Docking (IFD) approach. In IFD protocol, ligands were docked

into the rigid protein using soften potential docking in the Glide program with the van der Waals radii scaling of 0.8 for both proteins and ligand nonpolar atoms [32]. Energy minimization was carried out using OPLS-2005 force field with implicit solvation model until default criteria were met [33]. Rigid receptor peptide complex cordially estimates ligands within binding site and scoring functions will provide conformations based on interactions. But both protein peptide complex and ligand in flexible condition with multiple protein conformations will provide the maximum possibility of accurate interactions. This is made possible through combined protocol of prime and Glide through induced fit docking. The final best 5 compounds on high-throughput screening were further refined through IFD. Here, each docked conformer in previous step was subjected to side-chain and backbone refinements through prime. Different possible conformations are generated through prime and multiple conformations are docked through glide. The refined complexes were ranked by prime energy, and the receptor structures within -30 kcal/mol of the minimum energy structure were passed for a final round of Glide docking and scoring. The side-chain orientations have been performed automatically with inclusion of prime in IFD [34]. An IFD score that accounts for both the substrate bound protein–ligand interaction energy and the total energy of the system was calculated.

Binding Energy Calculation

The free energy of binding is calculated for selected screened compounds using the Prime/MM-GBSA method [35]. This simulation was carried out using the OPLS-2005 force field and GBSA continuum model in Prime version 3.0 from Schrodinger. Prime uses a surface generalized Born (SGB) model employing a Gaussian surface instead of a van der Waals surface for better representation of the solvent accessible surface area [36].

The binding free energy, $\Delta G_{bind,}$ was calculated using the following equations.

$$\Delta G_{bind} = \Delta_E + \Delta G_{solv} + \Delta G_{SA} \quad (1)$$

$$\Delta_E = E_{complex} - E_{protein} - E_{ligand,} \quad (2)$$

Where $E_{complex}$, $E_{protein}$, and E_{ligand} are the minimized energies of the protein-inhibitor complex, protein, and inhibitor, respectively.

$$\Delta G_{solv} = G_{solv}\ (complex) - G_{solv}\ (protein) - G_{solv}\ (ligand), \quad (3)$$

Where G_{solv} (complex), $G_{solv\ (}$protein), and G_{solv} (ligand) are the solvation free energies of the complex, protein, and inhibitor, respectively.

$$\Delta G_{SA} = G_{SA}\ (complex) - G_{SA}\ (protein) - G_{SA}\ (ligand), \quad (4)$$

Where G_{SA} (complex), G_{SA} (protein), and G_{SA} (ligand) are the surface area energies for the complex, protein, and ligand, respectively.

Molecular dynamics simulation

The molecular dynamics simulations have been carried out for all native type as well as mutant forms of LPNTG peptide bound SrtA complexes and docked structures of peptide blocker compounds bound with LPNTG SrtA complexes to understand protein peptide interactions and its stability in dynamic state using Desmond molecular dynamic system with OPLS2005 force field. The protein complexes with negative charges (-3) were solvated in an orthorhombic box with TIP3P water molecules, overlapping water molecules were deleted and the systems neutralized with Na+ ions. [37], whereas the orthorhombic boundary condition of system was X=59.49Å, Y=61.97Å and Z=60.64 Å and the system contains 20705 number of atoms in the simulation box. While the solvated structure was energy minimized using the steepest descent method to remove close contacts, terminating when maximum force is found smaller than 100 KJ/mol^{-1}/nm-^{1}. The distance between the box wall and complexes was set to greater than 10 Å to avoid direct interaction with its own periodic image. All systems were subjected to up to 100 steepest descent energy minimization steps before thermalization, for a maximum force of more than 100 KJ/mol^{-1}/nm^{-1} and the temperature was controlled through Nosé–Hoover thermostat dynamics with a damping coefficient of 2 ps^{-1} for equilibration and production runs. After thermalization, MD simulation was run at the isothermal isobaric (NPT) ensemble at a constant temperature (300 K) and pressure (1 bar) with a time step of 2 fs and the relaxation time was applied between 0.1 and 0.4 fs. NVT simulation was carried out for 1ns and the simulated conformers were equilibrated for 20 ns of the time scale [38-39]. The long range electrostatic interactions were computed by particle-mesh Ewald method and van der Waals (VDW) cut-off was set to 9 Å. The Cα-RMSD, root mean square fluctuation (RMSF) and hydrogen bond interactions for SrtA-LPNTG and peptide blocker compounds bound LPNTG SrtA complexes were calculated for the entire simulation trajectory with reference to their respective first frames. The distance between Leu NH_3 (H1, H2, H3) atoms of LPNTG substrates for the entire complexes forming hydrogen bonding interaction with SrtA binding site residues was calculated and plotted throughout 20ns time scale of simulations.

Screened peptide blocker ligand physico-chemical properties

The identified best screened compounds were assessed for their drug likeness behavior through evaluating the pharmacokinetic parameters required for their absorption, distribution, metabolism and excretion (ADME) using QikProp (v4.4) module of Schrodinger software [40-41]. Screened compounds were neutralized before being used by QikProp [42], because this program was unable to neutralize the structure and it was processed in normal mode predicted principle descriptors and physiochemical properties of all the compounds with detailed analysis of the log P (octanol/water), log HERG (HERG K^+ channel blockage) and percent of human oral absorptions, while accurate prediction of ADME properties prior to experiment procedures can eliminate unnecessary testing of compounds.

Results and Discussion

Molecular modeling and validations

The main aspects in homology modeling are choosing the appropriate template and multiple sequence alignment between the target and template sequence. In this homology model is generated for the catalytic domain of *S. mutans* SrtA using two template sequences of SrtA enzyme, namely those of *S. agalactiae* with 66% identity (**3RCC**) and *B. anthracis* (**2KW8**) with 36% identity. Even though the identity between target and template was comparatively low the functions of the sequences were found to be unique, so the both template sequences were chosen to be suitable templates. Meanwhile, the obtained *S. mutans* homology model superposes well with template, and the overall Cα RMSD was found to be **0.951**Å using chimera. The secondary structure of the predicted SrtA structure is composed of 2 helix and 8 beta-sheets [α1 (91-96), α2 (134-136), β1 (66-80), β2 (81-90), β3 (97-114), β4 (115-133), β5 (137-150), β6 (151-176), β7 (177-191) and β8 (195-202) (supplementary information figure S1). To evaluate the quality and reliability of predicted model, the least energy model is subjected to several validations. In Ramachandran plot, 83.5% of residues were found to be fully present in allowed region, 14.8% in additionally allowed region, 1.7% in generously allowed region and 0.0% residue in disallowed region. The model validation results point out that the backbone dihedral angles of ψ and φ angles in model are reasonably accurate (supplementary information figure S2). In addition to that energy calculation of Non-Local Environment (NLE) of each heavy atom on a protein chain was performed using Atomic Non-Local Environment (ANOLEA) and energy value for each amino acid of the protein is shown in supplementary information figure S3. Furthermore, the potential errors in predicted 3D models of protein were checked using PROSA server and the overall quality of model and deviation of total energy in the random conformation of predicted model with

respect to energy distribution was indicted in Z-score (supplementary information figure S4 A, B), while the Z-score of the template 2KW8, 3RCC is -6.41, -5.19kcal/mol, respectively, and target is -6.22kcal/mol which indicates that the model structure is similar to template structure. From these results, it is confirmed that predicted model is more reliable and accurate based on stereo chemical, and overall quality factors are shown in figure 2a. Thus, the final refined model is subjected for other calculations of molecular modelling.

Molecular dynamics of SrtA interaction with LPNTG substrate

To study the role of universally conserved Leu residue of sorting signal in changing the conformation of the enzyme-substrate structural complex. We first docked the extended LPNTG pentapeptide into the binding site of SrtA homology model (figure 2b). The LPNTG-binding motif was used because *S. mutans* biofilm forming surface proteins possesses this as a motif and acts as a substrate for SrtA. The docked LPNTG complex showed very good interactions with residues of Asn91, His118, Glu165, Arg192 and Glu168. As a result, the pentapeptide NH_3 group of Leu residue forms hydrogen bond interaction with SrtA Asn91 and His118 residues as shown in figure 2c. Molecular simulation studies of SrtA were carried out in the absence (designated ApoSrtA) and the presence of LPNTG (designated SrtA-LPNTG). The time-dependent Cα atom RMSD values for both ApoSrtA and SrtA-LPNTG complex were calculated to assess the conformational stability of the protein complex during MD simulation, which showed a stable conformation of protein complex throughout the 20 ns time scale after attaining its equilibrium state as represented in Figure 3.

Invariant Leu residues exploit specific effects on Dynamics of SrtA

To explore the specific role of Leu substrate residue in directing the conformational changes of the protein complex, we performed MD simulation of SrtA-substrate complexes in which conserved substrate Leu residue NH_3 group of amino H atoms were replaced by a methyl functional group. Single mutant forms (Leu NH_3 (H1...CH_3), Leu NH_3 (H2...CH_3), Leu NH_3 (H3... CH_3) and double mutant forms Leu NH_3 (H1-H2...CH_3) were generated to confer a critical role of this residue in the conformational dynamics of enzyme substrate complexes. The Cα atom RMSD of mutated SrtA-LPNTG complexes versus time showed distinct deviation in dynamics of the SrtA compared to native forms (Figure 4 and supplementary information figure S5) and consequently affected the specificity of the substrate recognition. The distance between H atoms of NH_3 group of Leu substrate residue interacting with binding site SrtA residue was calculated and plotted through 20 ns

simulations as given in Figure 5. Comprehensively, these results indicate that the mutant forms of Leu substrate residue seem to alter the stability of the complex and play a direct role in conformational transition of the enzyme. Eventually the docking score and energy values of wild type as well as mutant forms of LPNTG substrate also specified that mutant LPNTG forms change the conformation of SrtA structure (Supplementary information Table S1). However, hydrogen bond interactions of protein substrate complexes are given in supplementary information figure S6 and also the root mean square fluctuation plot for each complex is represented in supplementary information figure S7 (A, B).

Molecular electrostatic potential analysis

We assumed that it is important to understand the surface electronic properties of LPNTG substrates to comprehend the difference in electrical charge between native and mutant forms. Accordingly, the LPNTG substrates MESP, HOMO-LUMO parameters, solvation energy and free energy were analyzed and tabulated in Table 1. Both HOMO and LUMO energies are small, ranging between -0.23423 to -0.19481 and -0.01976 to -0.01596 eV respectively, indicating the fragile nature of bound electrons. HOMO and LUMO sites were plotted onto the surface of LPNTG substrates and shown in Figure 6. The MESP plotted onto the constant electron density surface for LPNTG substrates showed that most electropositive potential region (blue color) near Leu NH_3 of the native and mutant form of peptides are given in Figure 7. Thus, DFT analysis revealed the difference in their charge of LPNTG substrates surface.

Free energy perturbation calculation of mutant LPNTG peptides

We performed free energy perturbation (FEP) calculation to know the free energy difference of the mutant LPNTG substrates. The calculated free energy differences of mutant LPNTG-H1, LPNTG-H2 are ΔG 25.0737+-0.0413, 25.3201+-0.0384 kcal/mol, respectively. While FEP simulation of mutant LPNTG-H1 substrate showed a slight difference in energy value when compared with that of mutant LPNTG-H2 substrate, but these mutations on LPNTG peptides significantly affect the enzyme substrate interaction.

Virtual Screening of LPNTG peptide blocking compounds

The combined approach of Funnel-based virtual screening and IFD has been carried out to find potential lead compounds(supplementary information figure S8), which act as a peptide blocker for the inhibition of SrtA-mediated transpeptidation, while the compounds

from zinc database are docked into the binding site of LPNTG bound receptor and the best compounds with specific interaction on leucine of LPNTG peptide bound protein complex were selected based on the GlideScore and energy level values through virtual screening final state XP docking method (supplemental information Table S2). Further selected hit compounds were redocked through flexible ligand and receptor using IFD method and the results of IFD for the best compounds are given in Table 2, which distinctly shows that selected screened compounds precisely interacted with the leucine H1 of LPNTG substrate and Asn91, Arg192, Thr95, Ser130, Pro164 and Thr185 amino acids of SrtA enzyme with satisfactory score values and energy levels are shown in Figure 8. As this top hit peptide blocker compounds of docking calculations show much correlation in terms of energy with both binding and docking. Finally, the 5 lead compounds based on their interactions and docking score were taken ahead for molecular dynamics simulation studies and prediction of ADMET analysis.

MMGBSA calculation of peptide blockers-LPNTG bound SrtA complex

We estimated the binding-free energies of peptide bound SrtA complex with top screened compounds using an *in silico* molecular mechanics/generalized Born surface area (MMGBSA) method. The calculated free energies of screened compounds bound with SrtA complex range from -38.251439 to -52.461751 kcal/mol (ΔG_{bind} = -38.251439 kcal/mol to -52.461751 kcal/mol) shown in Table 3. According to the energy components of the binding-free energies, the major favorable contributors to ligand are van der Waals and nonpolar solvation terms (ΔGsolv SA), whereas polar solvation (ΔGsolv GB) opposes binding. So, we are able to make plausible assumption of compounds with strong binding affinities with enzyme to be used in the studies of MD simulations and can be used to direct the development of novel LPNTG peptide blocker compounds

Molecular Dynamics Simulations of Peptide Blocker Compounds-Protein Complexes

To gain insight into the stability and dynamic properties of the Leu specific peptide blocker compounds bound with protein complexes, 20ns of MD simulations were performed. We assessed the stability and dynamic properties of the complexes during MD simulation and RMSD of Cα atoms was analyzed and plotted in a Figure 9, while the simulation results revealed that RMSD of the complexes showed distinct fluctuation compared to the LPNTG bound protein complex and suggesting that it was due to the presence of Leu specific ligand-

induced conformational changes in the peptide bound protein complex. The atomic distance between H atoms of Leu NH_3 substrate residue bound protein complexes and their interacting amino acids (H1-Leu89, H2-Asn91 and H3-His118) in binding sites of SrtA complexes showed distinct aberration in interaction distance throughout span of the molecular simulation studies which is shown in Figure 10. However, the RMSF of each complex and peptides is given in supplementary information figure S9. We herein clearly emphasized that screened compounds weaken the binding affinity of enzyme substrate complexes and thereby hinder SrtA-mediated transpeptidation reaction

ADME-Drug physiochemical properties

We evaluated the five selected screened compounds for the pharmaceutically relevant properties to check their drug-like behaviour through the analysis of pharmacokinetic parameters required for ADME (Absorption, Distribution, Metabolism and Excretion) using QikProp. The predicted important pharmacokinetic parameters of screened compounds satisfy the ADME properties are shown in Table 4. The TOPKAT module predicted that the selected screened compounds are exempt from skin irritations and carcinogenesis along with good partition coefficients (QPlogPo/w) values, which were critical for understanding of absorption and distribution of drugs within the body, ranged between 1.79 and 2.852. QPPCaco indicating cell permeability of compounds ranged from 145.966 to 343.357, where QPPCaco was a predicted apparent Caco-2 cell permeability in nm/s value, plays a key role in governing drug metabolism and it accesses to biological membranes. Overall, the percentage of human oral absorption for the compounds was in the range of 80.885 to 85.697% and all these pharmacokinetic properties are suited well within acceptable range and defined for human use. Therefore, it can be concluded that all the compounds have sufficient ADME properties and also possess drug-like properties.

Conclusion

In this study, the integrated molecular modeling methods were used to delineate roles of fully conserved Leu residue of LPXTG substrate in conformational attributes of enzyme substrate complex structure. Overall the results of mutation studies, MD simulation and MSEP analysis demonstrated the significant role of Leu residue of substrate in anchoring to *S. mutans* SrtA and thereby governing their distinct conformation modification in protein structure. Furthermore, we identified potential lead compounds, which specifically target the Leu residue of substrate as peptide blockers to block SrtA catalyze transpeptidation reactions

on the bacterial surface through structure-based virtual screening with docking simulation method. While MMGBSA binding energy values indicate stronger relative binding affinities of selected screened compounds towards target and ADME properties calculated are in the preferable ranges, so these selected compounds are predicted to have drug like behaviour with less toxicity. Thus, these results attribute a distinct role of Leu in changing the dynamics of enzyme substrate complex structure and also facilitate a new form for designing inhibitor against the drug target.

Acknowledgements: One of the author SKS thankfully acknowledge the Department of Biotechnology (DBT-India) for the research grant (DBT TWIN Project: BT/502/NE/TBP/2013). This paper was supported by the KU Research professor program of Konkuk University, Seoul, South Korea. This work was supported by the Energy Efficiency & Resources Core Technology Program of the Korea Institute of Energy Technology Evaluation and Planning (KETEP), granted financial resource from the Ministry of Trade, Industry & Energy, Republic of Korea (201320200000420).

Conflicts of Interest: The authors declare there is no conflict of interest.

References

1. K. Hojo, S. Nagaoka, T. Ohshima and N. Maeda, *Journal of dental research* 2009, *88*, 982-990.
2. S. Hasan, M. Danishuddin, M. Adil, K. Singh, P. K. Verma and A. U. Khan, *PloS one* **2012**, *7*, e40319.
3. P. E. Petersen, *Community Dentistry and oral epidemiology* **2003**, *31*, 3-24.
4. Y.-H. Li, P. C. Lau, N. Tang, G. Svensäter, R. P. Ellen and D. G. Cvitkovitch, *Journal of bacteriology* **2002**, *184*, 6333-6342.
5. J. R. Scott and T. C. Barnett, *Annu. Rev. Microbiol.* **2006**, *60*, 397-423.
6. L. A. Marraffini, A. C. DeDent and O. Schneewind, *Microbiology and Molecular Biology Reviews* **2006**, *70*, 192-221.
7. A. Mandlik, A. Swierczynski, A. Das and H. Ton-That, *Trends in microbiology* **2008**, *16*, 33-40.
8. C. M. Levesque, E. Voronejskaia, Y.C. C. Huang, R. W. Mair, R. P. Ellen and D. G. Cvitkovitch, *Infection and immunity* **2005**, *73*, 3773-3777.
9. S.-J. Ahn, S.-J. Ahn, Z. T. Wen, L. J. Brady and R. A. Burne, *Infection and immunity* **2008**, *76*, 4259-4268.
10. A. Swaminathan, A. Mandlik, A. Swierczynski, A. Gaspar, A. Das and H. Ton-That, *Molecular microbiology* **2007**, *66*, 961-974.
11. H. Ton-That, L. A. Marraffini and O. Schneewind, *Biochimica et Biophysica Acta (BBA)-Molecular Cell Research* **2004**, *1694*, 269-278.
12. H. Ton-That, K. F. Faull and O. Schneewind, *Journal of Biological Chemistry* **1997**, *272*, 22285-22292.
13. P. Huang, P. Hu, S. Y. Zhou, Q. Li and W. M. Chen, *Current microbiology* **2014**, *68*, 47-52.
14. G. K. Paterson and T. J. Mitchell, *Trends in microbiology* **2004**, *12*, 89-95.
15. P. Cossart and R. Jonquières, *Proceedings of the National Academy of Sciences* **2000**, *97*, 5013-5015.
16. T. Biswas, V. S. Pawale, D. Choudhury and R. P. Roy, *Biochemistry* **2014**, *53*, 2515-2524.
17. T. Igarashi, E. Asaga and N. Goto, *Oral microbiology and immunology* **2004**, *19*, 102-105.
18. S. A. Sehgal, N. A. Khattak and A. Mir, *Theor. Biol. Med. Model* **2013**, *10*, 1-13.

19. Q. Qin, Q. Kaas, L. Zhang, K. Xu, N. Li, W. Zheng and Q. Lai, *Plant Molecular Biology Reporter* **2013**, *31*, 109-119.
20. M. y. Shen and A. Sali, *Protein science* **2006**, *15*, 2507-2524.
21. D. Sengupta, D. Verma and P. K. Naik, *Journal of biosciences* **2007**, *32*, 1307-1316.
22. R. A. Laskowski, J. A. C. Rullmann, M. W. MacArthur, R. Kaptein and J. M. Thornton, *Journal of biomolecular NMR* **1996**, *8*, 477-486.
23. M. Pawlowski, M. J. Gajda, R. Matlak and J. M. Bujnicki, *BMC bioinformatics* **2008**, *9*, 403.
24. M. R. M. Hussain, N. A. Shaik, J. Y. Al-Aama, H. Z. Asfour, F. Subhani Khan, T. A. Masoodi, M. A. Khan and N. S. Shaik, *Gene* **2012**, *508*, 188-196.
25. N. Guex and M. C. Peitsch, *electrophoresis* **1997**, *18*, 2714-2723.
26. C. Selvaraj, A. Omer, P. Singh and S. K. Singh, Molecular bioSystems, **2015,** *11,* 178-189.
27. T. Schulz-Gasch and M. Stahl, *Journal of molecular modeling* **2003**, *9*, 47-57.
28. N. Kus, I. Reva and R. Fausto, *The Journal of Physical Chemistry A* **2010**, *114*, 12427-12436.
29. Y. Zhao and D. G. Truhlar, *The Journal of Physical Chemistry A* **2005**, *109*, 6624-6627.
30. Jaguar, version 8.2, Schrodinger, LLC, New York, NY, 2013.
31. A. R. Muralidharan, C. Selvaraj, S. K. Singh, J. R. Sheu, P. A. Thomas and P. Geraldine, *Journal of chemical information and modeling*, **2015,** *55,* 1686-1697.
32. W. Sherman, T. Day, M. P. Jacobson, R. A. Friesner and R. Farid, *Journal of medicinal chemistry* **2006**, *49*, 534-553.
33. C. Selvaraj, S. K. Singh, S. K. Tripathi, K. K. Reddy and M. Rama, *Medicinal Chemistry Research* **2012**, *21*, 4060-4068.
34. C. Selvaraj, P. Singh and S. K. Singh, *Applied biochemistry and biotechnology* **2014**, *172*, 1790-1806.
35. J. Du, H. Sun, L. Xi, J. Li, Y. Yang, H. Liu and X. Yao, *Journal of computational chemistry* **2011**, *32*, 2800-2809.
36. D. Das, Y. Koh, Y. Tojo, A. K. Ghosh and H. Mitsuya, Journal of chemical information and modeling, **2009,** *49,* 2851-2862.
37. K. K. Reddy, P. Singh and S. K. Singh, *Molecular BioSystems* **2014**, *10*, 526-536.
38. C. Koshy, M. Parthiban and R. Sowdhamini, *Journal of Biomolecular Structure and Dynamics* **2010**, *28*, 71-83.

39. T. Hansson, C. Oostenbrink and W. van Gunsteren, *Current opinion in structural biology* **2002**, *12*, 190-196.
40. R. Kothapalli, A. M. Khan, A. Gopalsamy, Y. S. Chong and L. Annamalai, *PloS one* **2010**, *5*, e12494.
41. QikProp, version 4.4, Schrodinger, LLC, New York, NY, 2013.
42. N. Chauhan, A. S. Vidyarthi and R. Poddar, *Chemical biology & drug design* **2012**, *80*, 54-63.

Figure captions

Figure 1**: a,** Mechanistic role of SrtA-LPXTG Blockers. **b**, Mechanism of SrtA-LPXTG binding in the cell wall formation. **c**, Role of LEU residue in SrtA and LPXTG binding. d, Mutant site atoms present in the LEU residue.

Figure 2a: Three Dimensional structure of homology model *S. mutans* SrtA.

Figure 2b: Active site region focused with Pink colour surface indicate the substrate binding capacity of SrtA

Figure 2c: Ligplot 2D interaction of SrtA with LPNTG peptide

Figure 3: RMSD of Cα atoms of apo SrtA, SrtA-LPNTG complex (A, B) respectively.

Figure 4: Comparison of RMSD C-alpha atoms complex dynamics of native SrtA LPNTG complex with mutated LPNTG Peptide

Figure 5: The atomic distance between the atoms involved in hydrogen bond interaction of LPNTG peptide through MD simulations.

Figure 6: (I) Plots of the highest occupied molecular orbital (HOMO) profiles of native and mutated LPNTG peptide (A-E) (II) Plots of the lowest unoccupied molecular orbital (LUMO) profiles of native and mutated LPNTG peptide (A-E).

Figure 7: Computed Molecular electrostatic potential contours of native and mutated LPNTG peptides

Figure 8: Molecular interaction of peptide blocker compounds with LPNTG peptide bound protein complex.

Figure 9: Comparison of RMSD C-alpha atoms of SrtA-LPNTG complex to peptide blocker compounds bound with protein complex

Figure 10: The atomic distance variation between the atoms involved in hydrogen bond interaction of substrate Leu NH_3 and SrtA induced by screened compounds through 20 ns MD simulations (A-C).

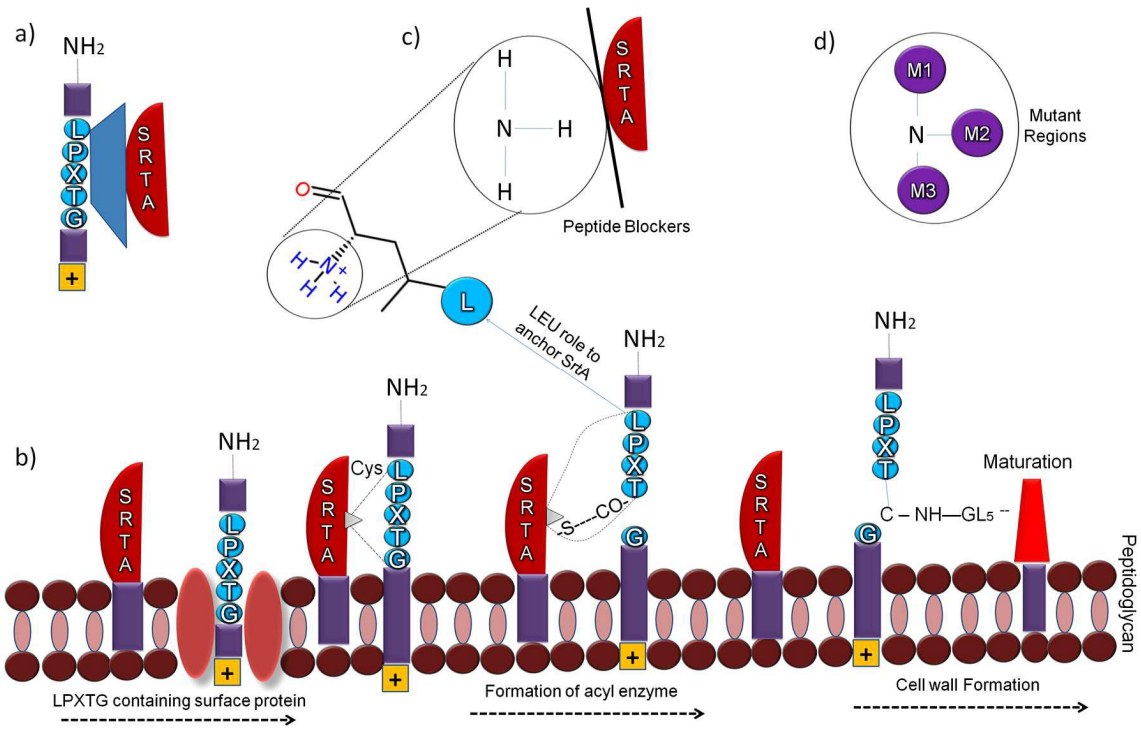

Figure 1**: a,** Mechanistic role of SrtA-LPXTG Blockers. **b**, Mechanism of SrtA-LPXTG binding in the cell wall formation. **c**, Role of LEU residue in SrtA and LPXTG binding. d, Mutant site atoms present in the LEU residue.

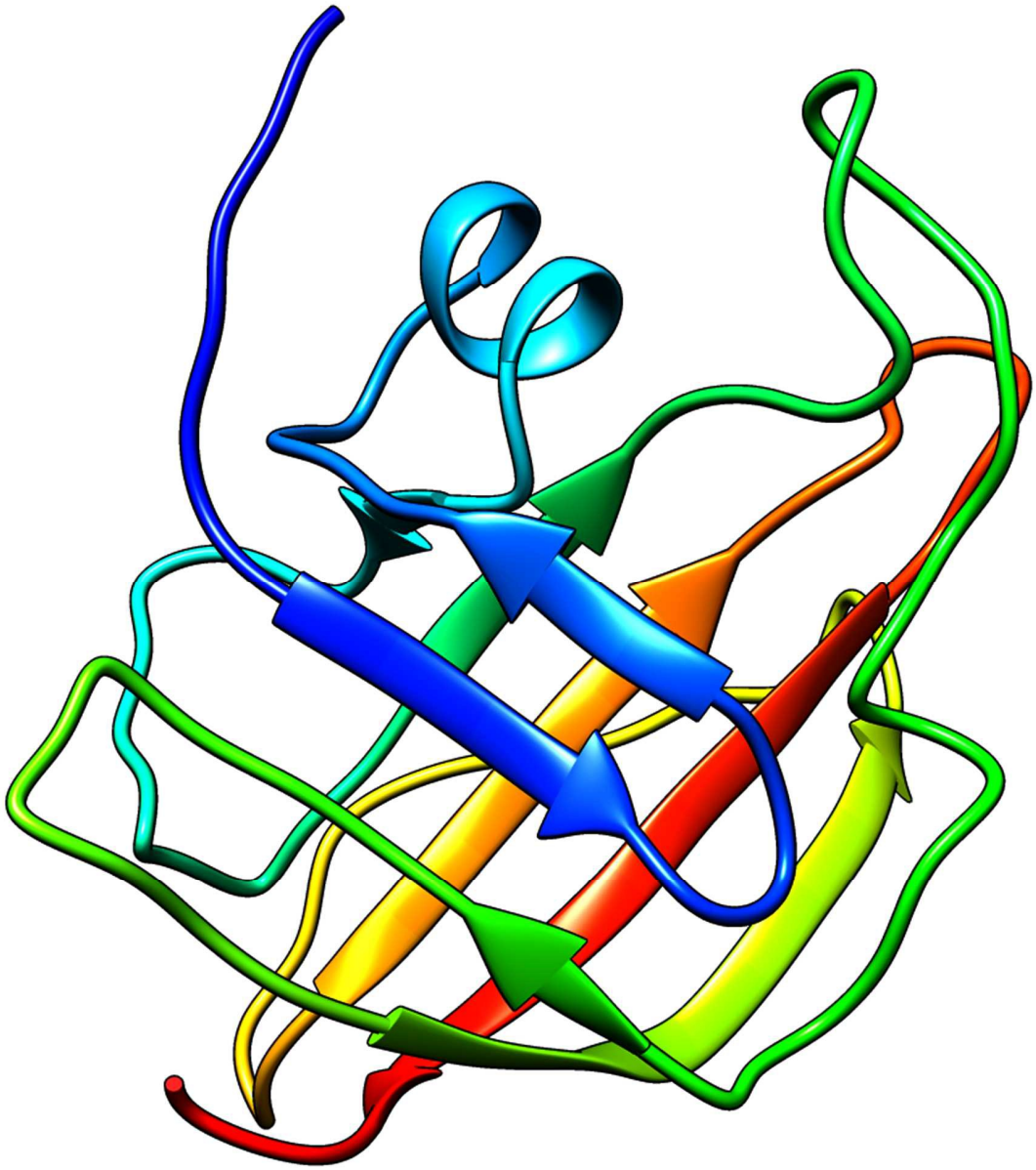

Figure 2a: Three Dimensional structure of homology model *S. mutans* SrtA.

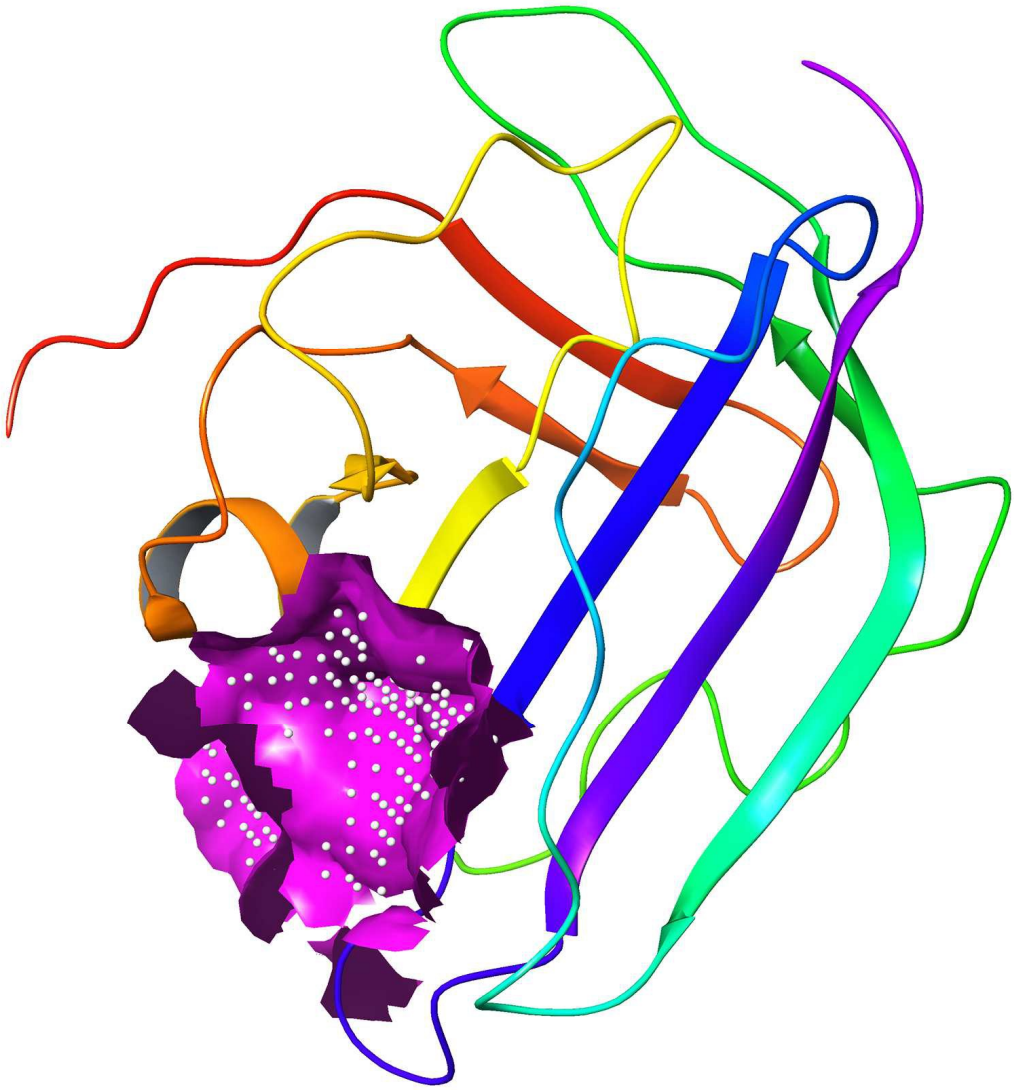

Figure 2b: Active site region focused with Pink colour surface indicate the substrate binding capacity of SrtA

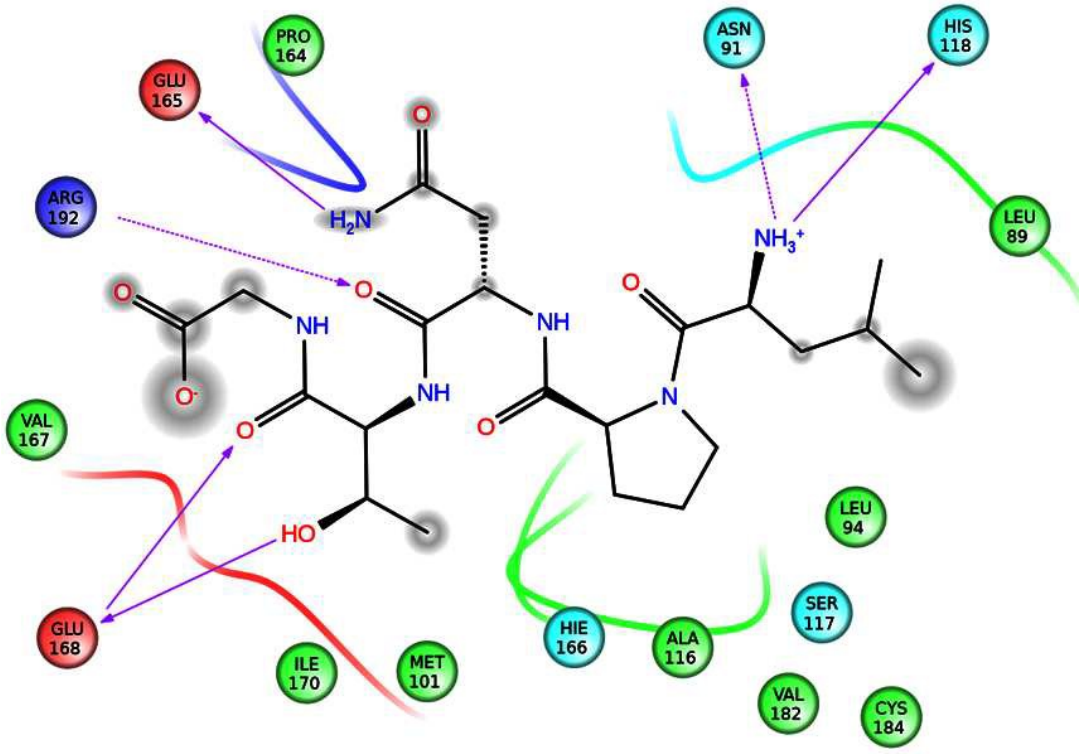

Figure 2c: Ligand 2D interaction of SrtA with LPNTG peptide

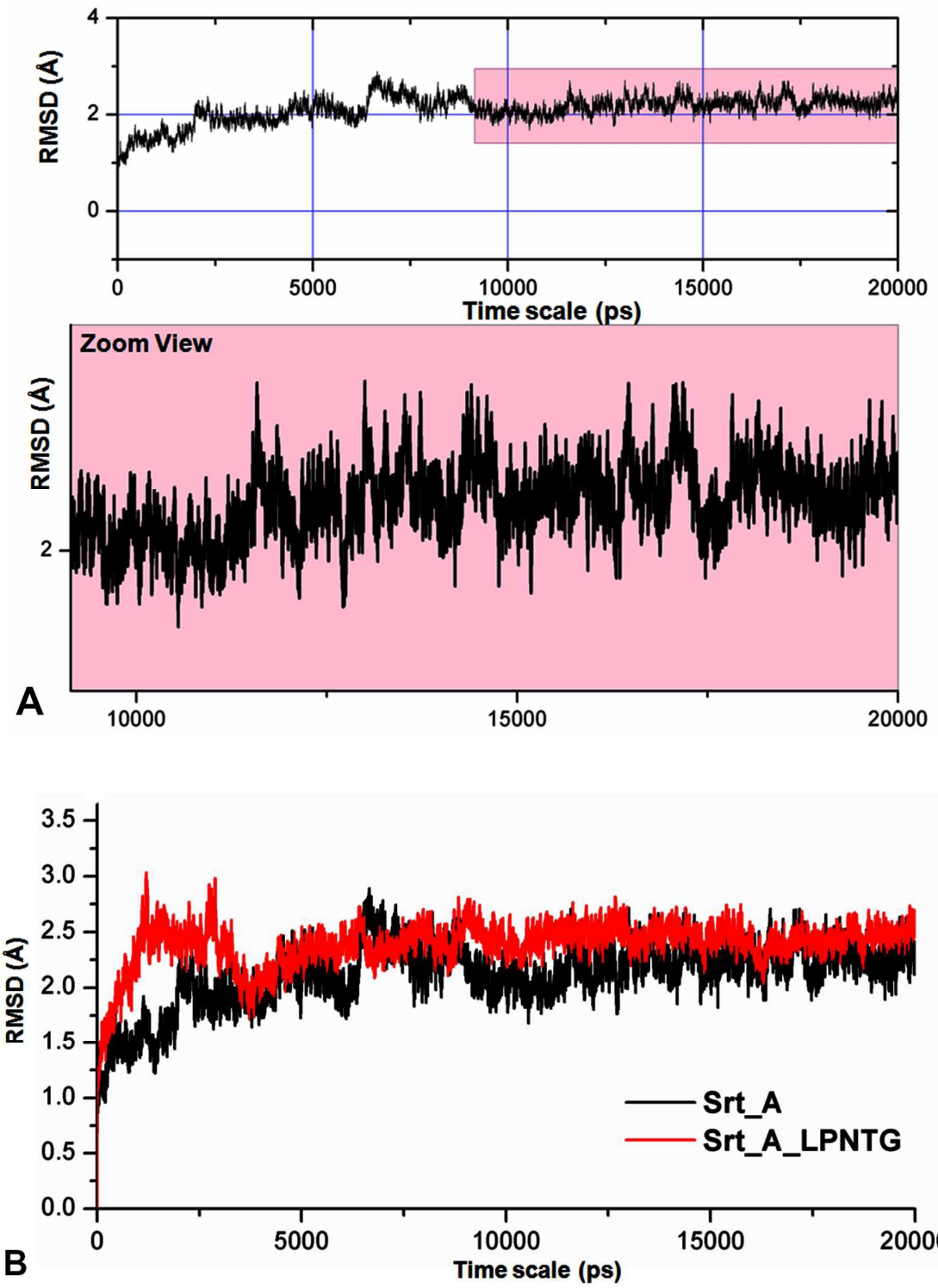

Figure 3: RMSD of Cα atoms of apo SrtA, SrtA-LPNTG complex (A, B) respectively.

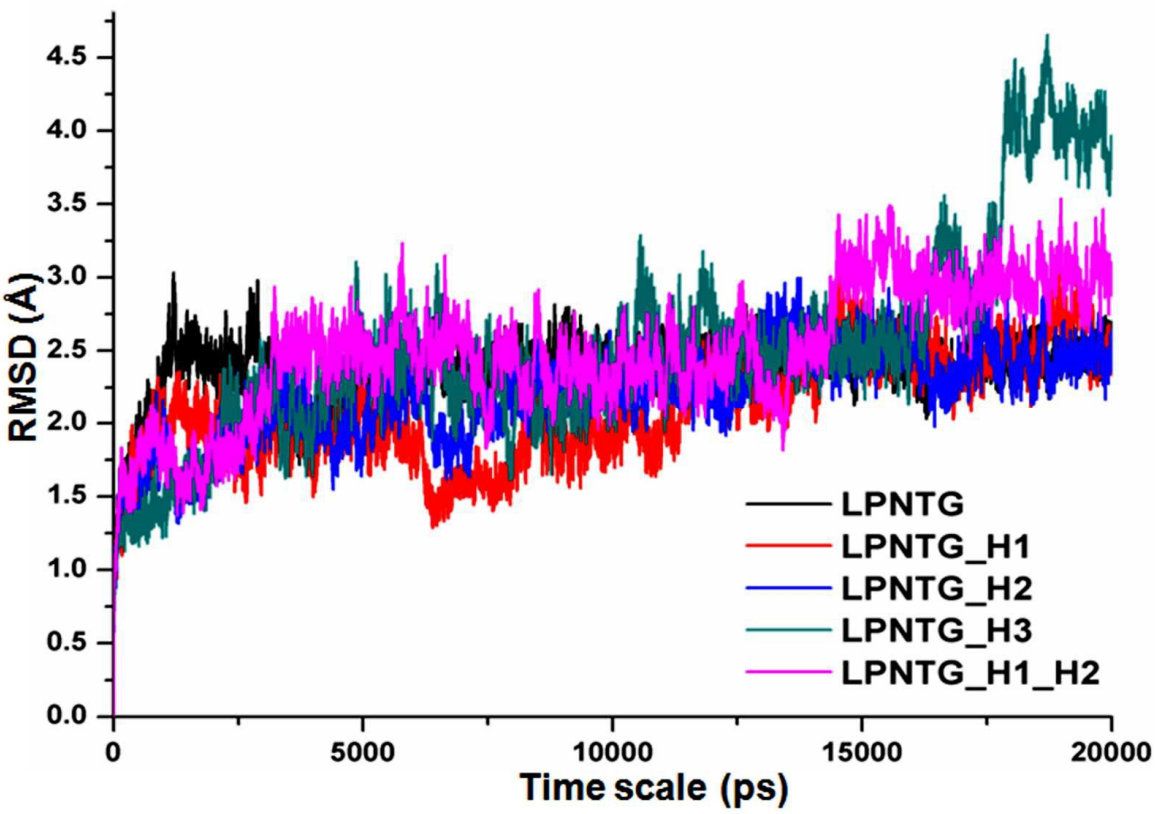

Figure 4: Comparison of RMSD C-alpha atoms complex dynamics of native SrtA LPNTG complex with mutated LPNTG Peptide

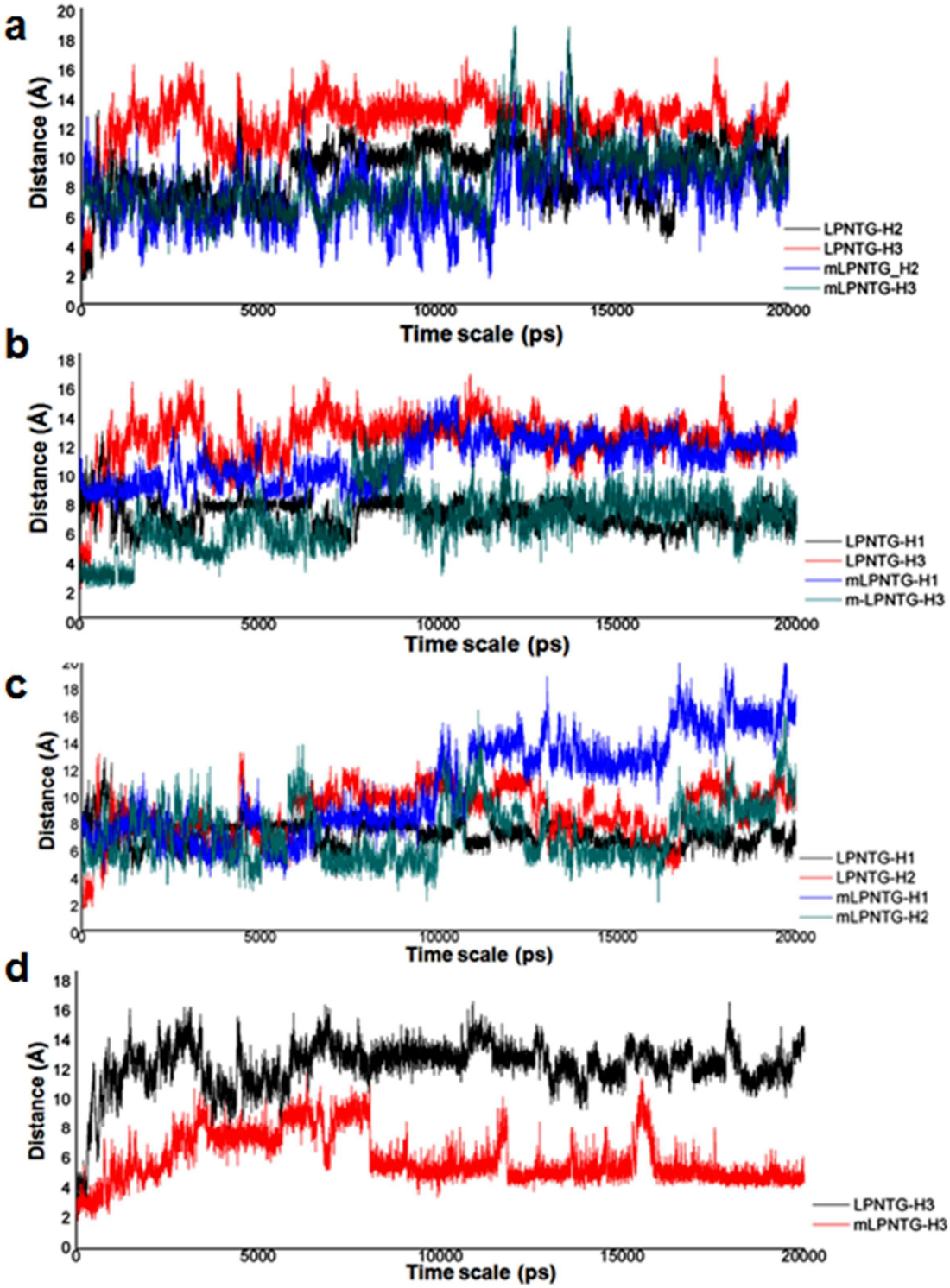

Figure 5: The atomic distance between the atoms involved in hydrogen bond interaction of LPNTG peptide through MD simulations.

A. Distance between hydrogen bonding binding site residues Leu89, Asn91 and His118 and mutated Leu NH_3—H1and H2 of LPNTG-H1 compared with native Leu NH_3—H1and H2 were depicted for the entire 20 ns simulation.

B. Distance between hydrogen bonding binding site residues Leu89, Asn91 and His118 and mutated Leu NH_3—H2 and H3 of LPNTG-H2 compared with native Leu NH_3—H2and H3 were depicted for the entire 20 ns simulation.

C. Distance between hydrogen bonding binding site residues Leu89, Asn91 and His118 and mutated Leu NH_3—H1 and H2 of LPNTG-H3 compared with native Leu NH_3—H1and H2were depicted for the entire 20 ns simulation.

D. Distance between hydrogen bonding binding site residues Leu89, Asn91 and His118 and mutated Leu NH_3—H3 of LPNTG-H1_H2 compared with native Leu NH_3—H3 were depicted for the entire 20 ns simulation

(I)

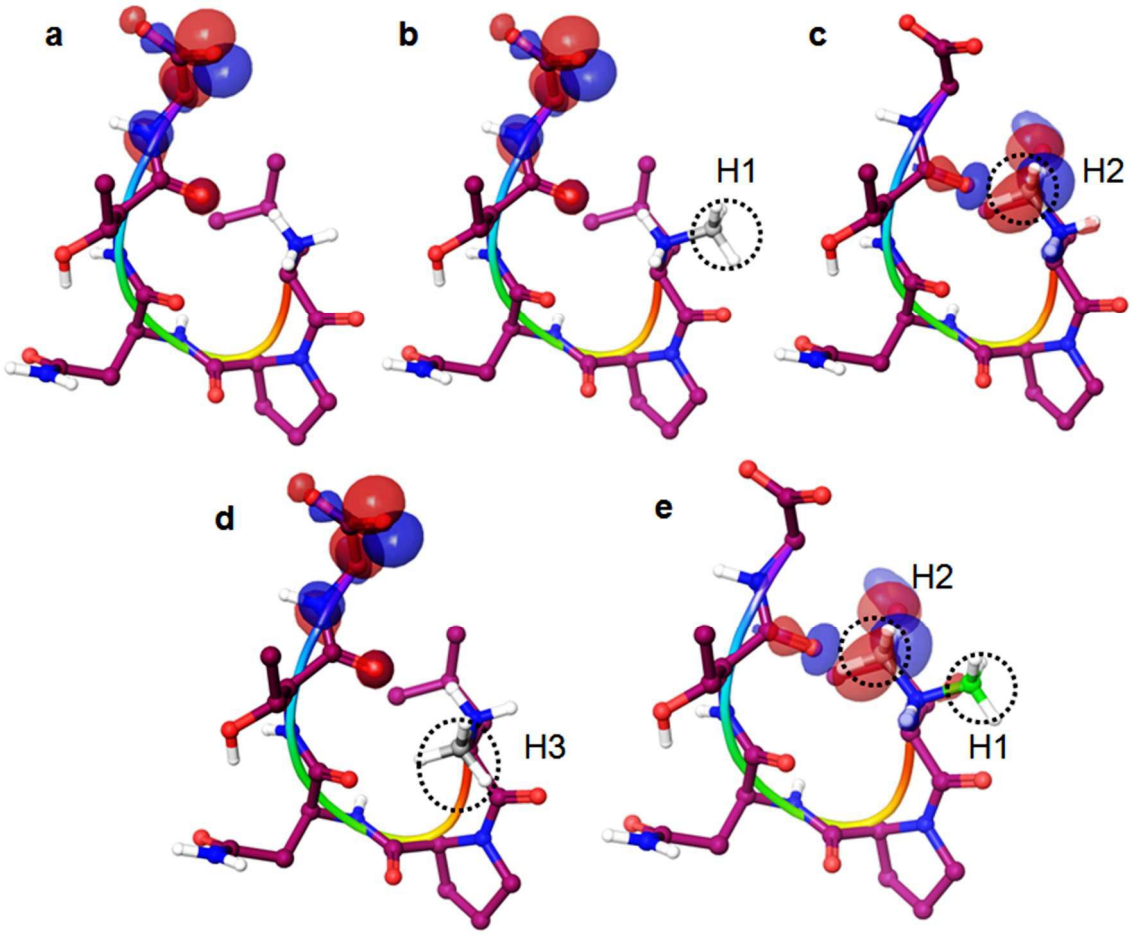

(II)

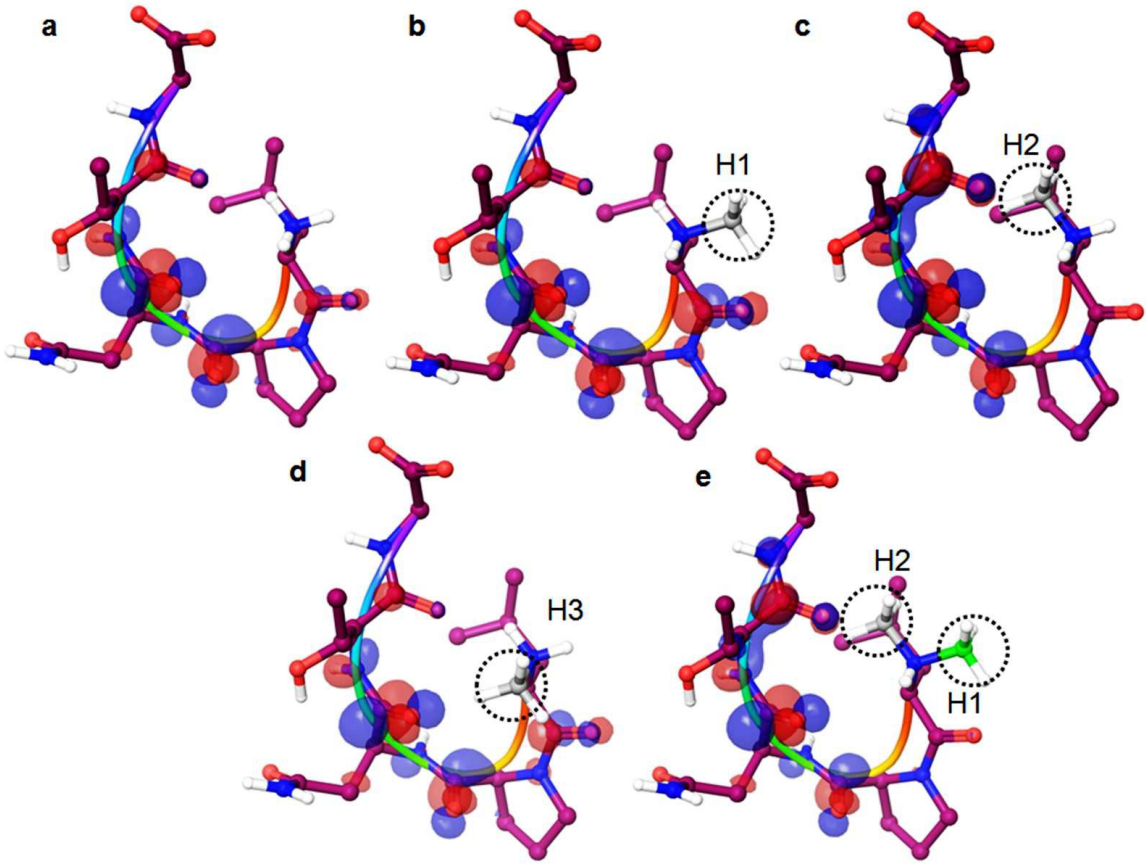

Figure 6: (I) Plots of the highest occupied molecular orbital (HOMO) profiles of native and mutated LPNTG peptide (A-E) (II) Plots of the lowest unoccupied molecular orbital (LUMO) profiles of native and mutated LPNTG peptide (A-E).

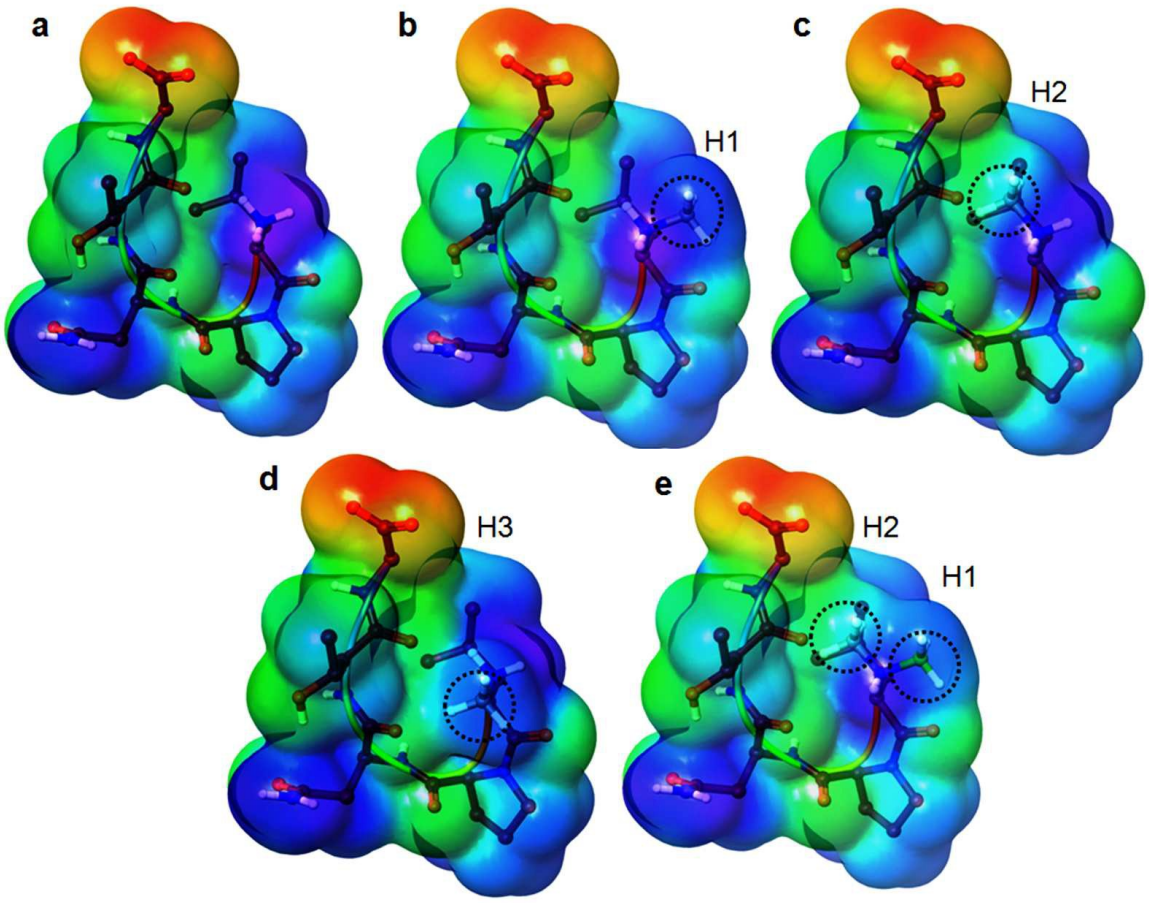

Figure 7: Computed Molecular electrostatic potential contours of native and mutated LPNTG peptides (A) LPNTG, (B) LPNTG_H1, (C) LPNTG_H2, (D) LPNTG_H3 and (E) LPNTG_H1_H2. [MSEP superimposed onto a surface of constant electron density showing the most positive potential region (deepest blue color) and the most negative potential region (deepest red color)].

The potential ranges according to color code: red (most negative) < orange<yellow<green<blue (most positive).

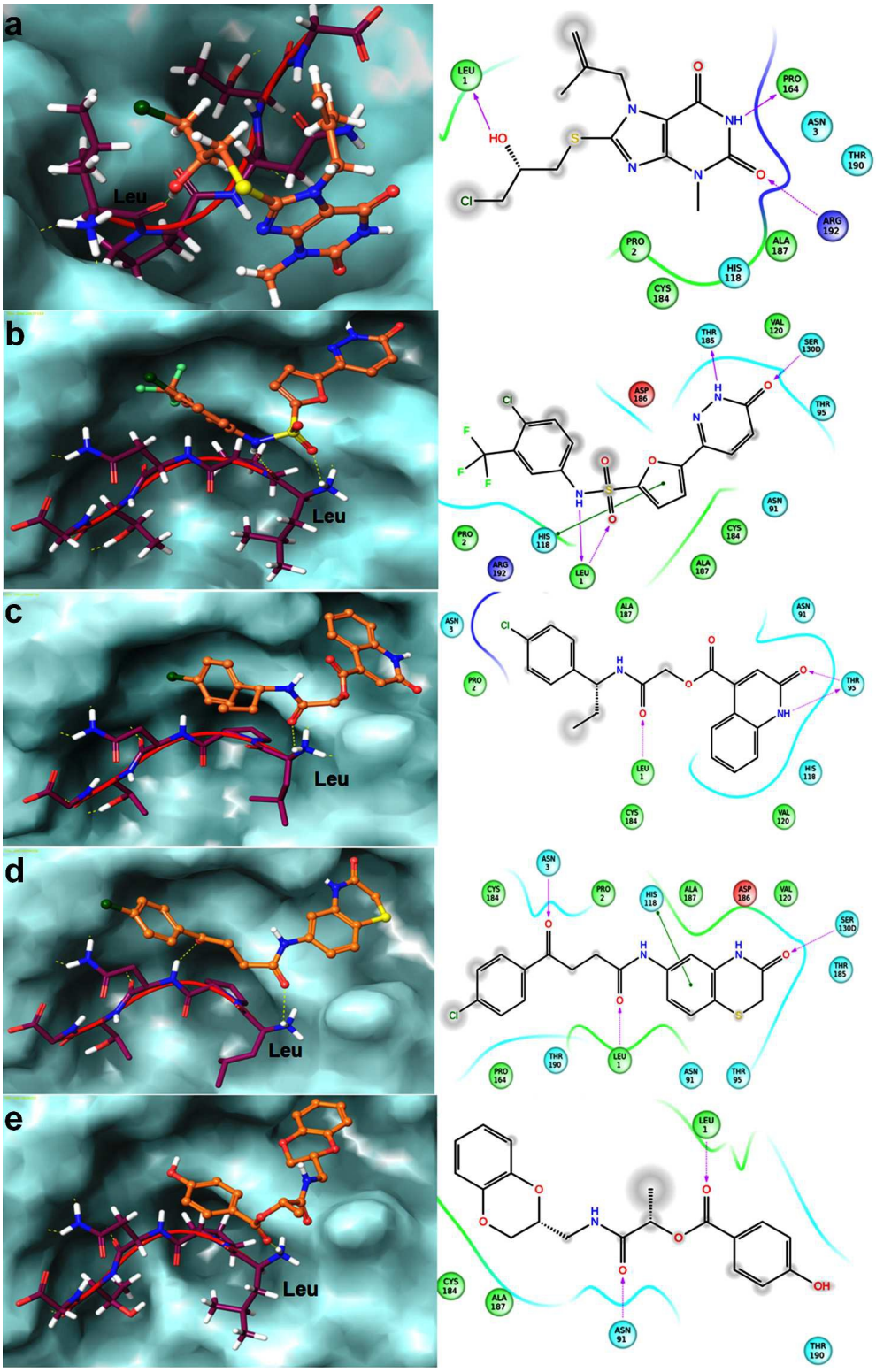

Figure 8: Molecular interaction of peptide blocker compounds with LPNTG peptide bound protein complex. **A**: Zn00266826, **B**: Zn20577153, **C:** Zn22946756, **D:** Zn24294906 and **E:** zn28130221

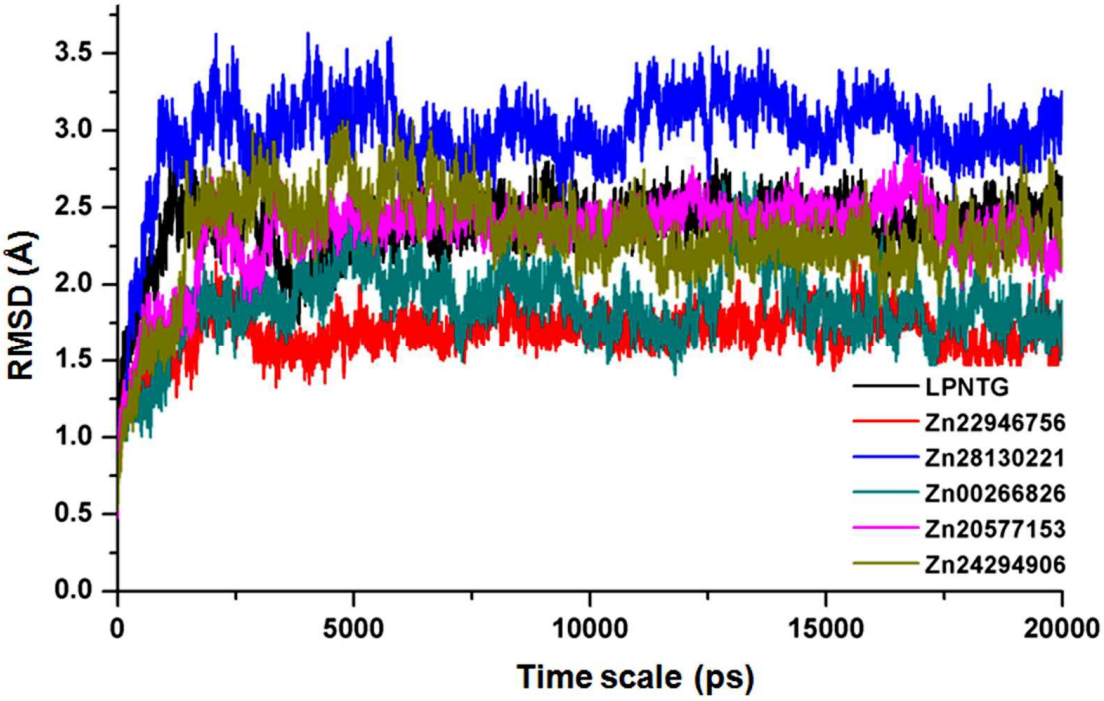

Figure 9: Comparison of RMSD C-alpha atoms of SrtA-LPNTG complex to peptide blocker compounds bound with protein complex

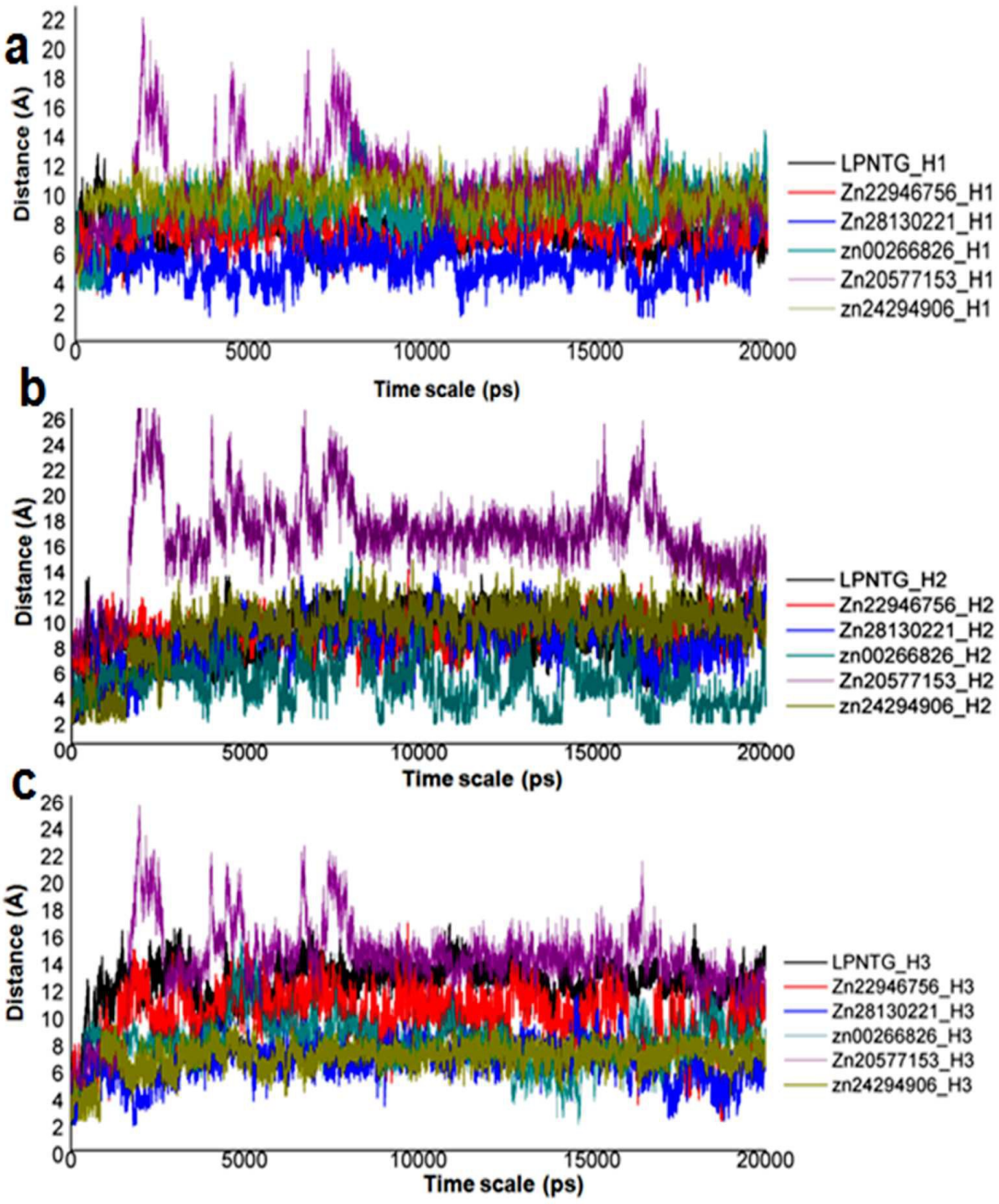

Figure 10: The atomic distance variation between the atoms involved in hydrogen bond interaction of substrate Leu NH_3 and SrtA induced by screened compounds through 20 ns MD simulations (A-C).

Table 1: Single point energy output values of LPNTG peptides

Peptide	HOMO	LUMO	Energy band gap	Solvation energy	Free energy	Most positive potential	Most negative potential
LPNTG	-0.23396	-0.01596	−0.24992	-0.159789	-47.627	125.4965	89.4269
LPNTG-H1-mutation	-0.23423	-0.01656	−0.21767	-0.14952	-46.521	126.1513	88.7616
LPNTG-H2-mutation	-0.19523	-0.01976	−0.17547	-0.144313	-44.187	121.5507	89.0621
LPNTG-H1-H2-mutation	-0.19481	-0.01975	−0.17506	-0.138261	-44.688	122.1	88.9121
LPNTG-H3-mutation	-0.23376	-0.01784	−0.21592	-0.147991	-47.772	125.512	88.8611

Table 2: Induced fit docking results for peptide blocker compounds with their interacting amino acids

Compounds	IFD score	H-bond	Atomic interaction between LPNTG peptide-ligand	Distance (Å)	Atomic interaction between SrtA-compounds	Distance (Å)
Zn22946756	-298.573	2	[Leu]=(H1)..OC	1.87	(Ser130C)=O...HN	1.85
Zn28130221	-295.524	3	[Leu]=(H1)...OC	2.13	(Pro164)=O...HO (Arg192)=H...OH	1.73 1.87
Zn00266826	-296.329	2	[Leu]= (O)...HO	2.02	(Ser130C)=O...HN	1.89
Zn20577153	-296.397	2	[Leu]=(O)...HN	2.11	(Ser130C)=O...HN	2.27
Zn24294906	296.064	2	[Leu]=(H1)...OC	2.20	(Arg192)=H...OC	1.93

Table 3: Binding free energy calculation results for the peptide blocker compounds bound with protein peptide complex [a].

Compound	ΔE			ΔG_{solv}	ΔG_{SA}	ΔG
	$\Delta G_{Coulomb}$ [b]	ΔG_{vdw} [c]	$\Delta G_{Covalent}$ [d]	ΔG_{SolGB} [e]	$\Delta G_{solLipo}$ [f]	ΔG_{bind} [g]
Zn22946756	-5.355409	-37.822797	3.533775	19.263455	-26.442055	-52.461751
Zn 28130221	-9.335167	-30.475839	3.832821	14.242725	-19.194568	-42.258278
Zn00266826	-4.689314	-28.735746	-1.123884	12.398631	-13.284758	-39.813269
Zn20577153	-3.518007	-28.992369	6.542836	11.997839	-18.604405	-38.251439
Zn24294906	-3.291265	-30.024151	3.806442	13.362994	-24.928764	-43.062317

[a] All energies are in kcal/mol

[b] Coulomb energy contribution to the binding free energy

[c] Van der Waals energy contribution to the binding free energy

[d] Covalent energy contribution to the binding free energy

[e] The generalized born electrostatic solvation energy contribution to the binding free energy

[f] The surface area due to lipophilic energy contribution to the binding free energy (nonpolar contribution estimated by solvent accessible surface area).

[g] Free binding energy

Table 4: ADME prediction of the peptide blocker compounds

Compounds (Molecular weight)	CNS	QPlogPo/w	QPPCaco	QPPMDCK	QPlogKp	Percent Human Oral Absorption	Skin Irritability	Carcinogen
Zn22946756 (398.845)	-2 (inactive)	2.852	200.568	331.154	-2.809	84.85	No	Non-carcinogen
Zn28130221 (357.362)	-2 (inactive)	2.283	343.357	244.566	-2.219	85.697	No	Non-carcinogen
Zn00266826 (344.815)	-2 (inactive)	1.79	267.903	224.506	-3.85	80.885	No	Non-carcinogen
Zn20577153 (419.762)	-2 (inactive)	2.618	145.966	501.925	-3.834	81.013	No	Non-carcinogen
Zn24294906 (374.841)	-2 (inactive)	2.392	205.233	375.178	-3.421	82.333	No	Non-carcinogen

Recommend value ranges are follows

CNS : Predicted central nervous system activity on a -2 (inactive) to + 2 (active) scale, QPlogPo/w: Predicted octanol/water partition coefficient (–2.0 – 6.5), QPPCaco: Predicted apparent Caco-2 cell permeability in nm/sec (<25 poor, >500 great), QPPMDCK: Predicted apparent MDCK cell permeability in nm/sec (<25 poor, >500 great), QPlogKp: Predicted skin permeability, log *K*p (–8.0 – –1.0), Percent Human Oral Absorption >80% is high, <25% is poor

Mechanistic Insights of SrtA-LPXTG Blockers targeting the transpeptidase mechanism in Streptococcus mutans

Chandrabose Selvaraj[1], Ramanathan Bharathi Priya[2], Jung-Kul Lee[1], Sanjeev Kumar Singh[2]*

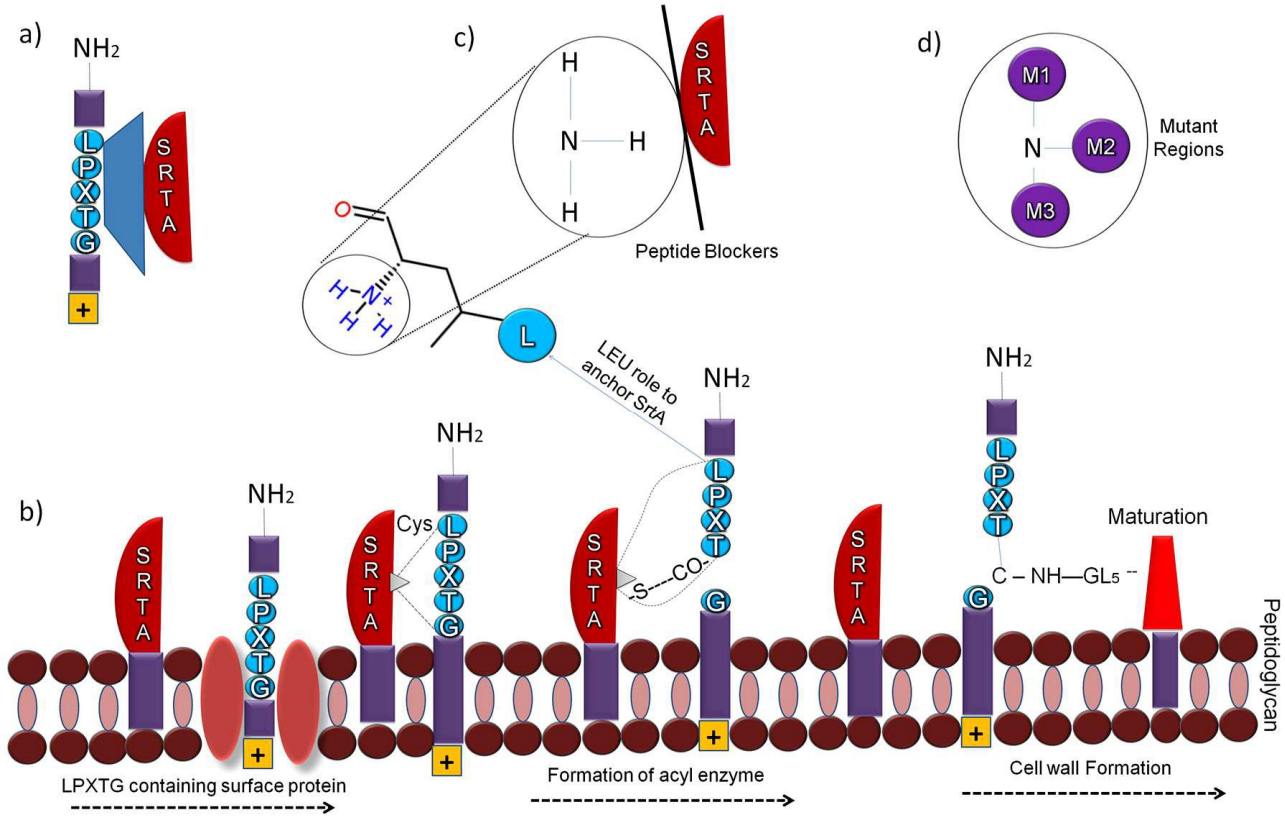

The SrtA-LPXTG interactions are playing a crucial role in the transpeptidation mechanism, cell wall formation and also in biofilm formation. Here the study involves the blocking the LEU interactions with SrtA will result in the SrtA inhibitors through different energy calculations and Molecular dynamics simulation studies.